# Reflection from an Unstable, Obliquely Irradiated Laser Plasma

R. Sigel, K. Eidmann, H. C. Pant,* and P. Sachsenmaier
*Max-Planck-Gesellschaft zur Förderung der Wissenschaften e. V., Projektgruppe für Laserforschung, 8046 Garching, West Germany*
(Received 18 November 1975)

An inhomogeneous plasma layer is unstable under intense laser irradiation as applied in laser fusion experiments. Experimental observations support the results of recent two-dimensional computer simulations.

The propagation of an electromagnetic wave in an inhomogeneous, plane plasma layer is well known within the approximation of linear optics. Solutions of the linear wave equation predict, for the general case of oblique incidence, specular reflection of the incident radiation with enhanced absorption for a $p$-polarized wave.[1] For intense light waves as applied in laser fusion experiments it is generally believed that the plasma layer becomes unstable under the action of the electromagnetic field structure. Though considerable experimental and theoretical effort has been devoted to the problem of wave propagation in an unstable plasma layer, no consistent picture has yet been arrived at.

Recently it became possible to simulate oblique incidence of a $p$-polarized light wave on an inhomogeneous plasma by two-dimensional particle-in-cell computer simulations.[2,3] The simulations suggest that instability of the plasma layer should result in strongly peaked scattering near the backscatter angle. Experiments tend to show corresponding behavior,[4-6] although widely differing experimental conditions and lack of reproducibility and completeness of data have resulted in a patchwork of observations which makes it difficult to isolate any common features. It therefore seems appropriate to report here experiments where the angular distribution of specular reflection, collimated backscatter, and second-harmonic (SH) generation, together with their time evolutions, are simultaneously recorded in single-shot experiments approaching the plane geometry of computer simulations. It then becomes obvious that the angular distribution seen in simulations indeed has its counterpart in real experiments. Imbedded in a set of data taken under identical conditions[4,5] and with the background of observations reported from other laboratories[6-8] the results seem to confirm a basic pattern of behavior with parallels between experiment and simulation which should help to unravel the experimental situation and narrow the range of relevant interaction mechanisms in laser-produced plasmas.

The experiments were performed on the Garching Nd laser facility ($\lambda = 1.06$ $\mu$m) with 5-nsec laser pulses of energy 0.1–20 J per pulse focused by a $f = 95$-mm aspherical lens (diam 75 mm). Plane targets of solid deuterium, plexiglass, carbon, copper, and tungsten oriented normally to the laser axis were used, the intensity on the surface being varied in the range $10^{12} \leq \Phi \leq 4 \times 10^{14}$ W cm$^{-2}$. To simulate oblique incidence of $p$-polarized radiation on the target, the laser beam, being linearly polarized with horizontal $E$ vector, was shifted horizontally to a position between the center and the left edge of the focusing lens. In addition, the right half of the lens was shielded from incident laser radiation by a sheet of cardboard with a straight vertical edge. Thus, it is essentially $p$-polarized light rays that impinge on the target with angles ranging from 0° (center of lens) to 25° (edge of lens). The angular distribution of backscattered radiation was studied by taking photographs of the full diameter of the focusing lens in the light of backscattered radiation.[4,5]

We discuss here two photographs obtained in a single laser shot onto a plane solid deuterium target [Figs. 1(a) and 1(b)]. In this case the target was in a defocused position with the focal spot about 200 $\mu$m in front of the target, resulting in an irradiated area of ~150 $\mu$m diameter at an intensity of approximately $10^{12}$ W cm$^{-2}$.

Under such conditions a pattern of reflected radiation is observed near the right edge of the lens, which is interpreted as specular Fresnel reflection from the plasma layer formed on the target surface. Obviously, the plasma layer remains plane and oriented normally to the optical axis during the laser pulse to such an extent that on a time-integrating photographic plate the reflected radiation appears about symmetric to the optical axis and well separated from the irradiated area in the left part of the lens. We note

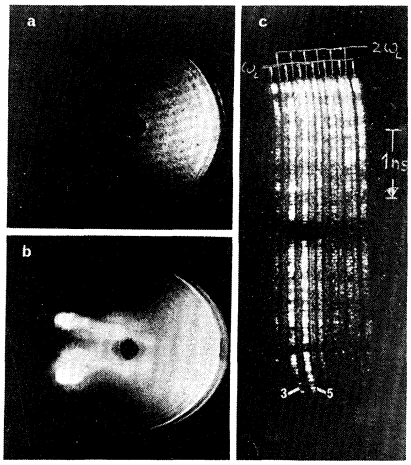


FIG. 1. Photographs of the focusing lens in the light of backscattered radiation. (a), (b) Time-integrated photographs at frequencies $2\omega_L$ and $\omega_L$, respectively. (c) Streak photograph with streak slit horizontal through the center of the lens. Channels three and five monitor collimated backscatter from two hot spots as seen in (b).

that formation of an approximately plane plasma layer is consistent with the large focal spot area forming the basis of Figs. 1(a) and 1(b).

It is apparent from Fig. 1(b) that the specular pattern is rather diffuse. In general, with varying target material, focus position, and intensity, the specular patterns were always diffuse, usually with an even broader angular range than in Fig. 1(b), and with local intensity variations of the incident beam being lost upon reflection. With some reservation this may be attributed to the inherent directional sensitivity of specular reflection to the shape of the plasma layer; x-ray pinhole photography and high-speed photography show that, in general, the target surface may already be considerably deformed during the laser pulse by crater formation.[9] Whether there is a deeper cause of blurring of specular reflection, namely reflection from a plasma layer which becomes rough during the interaction, will be the subject of a separate investigation.

In the left part of the lens collimated backscatter is observed in the form of four bright spots. Their spatial distribution is impressed by the "hot spots" which are present in the incident beam, and is, in contrast to specular reflection, not sensitive to the particular conditions of a laser shot. The high degree of accuracy with which the incident light rays are retraced has been demonstrated explicitly in Ref. 4.

For completeness and to demonstrate the connection with a previous investigation of SH production,[5] Fig. 1(a) shows the distribution of SH radiation obtained in the same laser shot. As discussed in Ref. 5, SH radiation should accompany specular reflection of $p$-polarized radiation.

The temporal evolution of the time-integrated patterns of Figs. 1(a) and 1(b) was followed by imaging the focusing lens on the slit plane of an ultrafast Electro-Photonics streak camera, with the streak slit extending horizontally through the center of the lens image as shown in Figs. 1(a) and 1(b). A special filter was constructed from 2-mm-wide strips of Schott RG 1000 and BG 18 filter glass. Glued together to form a plate with alternating strips, this filter was placed in the slit plane, thus dividing the field of view into thirteen channels alternately transmitting scattered radiation with frequenceis $\omega_L$ and $2\omega_L$. A typical streak photograph is shown in Fig. 1(c). For technical simplicity it was taken with a plane copper target under conditions (focused for maximum reflection through the lens with an intensity of $\Phi \simeq 10^{14}$ W cm$^{-2}$ on the target surface) where previous checks had shown that essentially the same patterns as shown in Figs. 1(a) and 1(b) are produced.

Inspection of Fig. 1(c) shows that SH radiation is preferentially emitted in the specular direction in agreement with the time-integrated Fig. 1(a). Maximum emission of SH radiation and specularly reflected laser radiation also occurs simultaneously as expected (actually during the first 1–2 nsec of the pulse). Channels three and five monitor collimated backscatter from the spots located in the left part of the lens [compare Fig. 1(b)]. In the following we ignore the slow, i.e. nanosecond, variation of the observed intensities, which is most probably connected with the time variation of the gasdynamic parameters of the plasma layer. Instead we concentrate on the high-frequency modulation seen in Fig. 1(c). It is observed that the scattered radiation fluctuates in time with single spikes being resolved down to a duration of $\Delta\tau \simeq 30$ psec, the time resolution of the camera in the present mode of operation. These fluctuations are basically due to fluctuations already present in the incident beam.

The important point is that individual spikes produce both modes of scattering, specular and collimated. Such a fast transition (<30 psec) excludes macroscopic deformation of the plane, specularly reflecting plasma layer as the cause for collimated backscatter. This is because generation of the pronounced spots of collimated

backscatter requires a coherent source with a minimum diameter which can be estimated by a simple diffraction argument as $d \gtrsim \lambda f/R$. For a typical hot-spot radius $R \approx 3$ mm in the plane of the lens [Fig. 1(b), left part] one finds $d \gtrsim 3 \times 10^{-3}$ cm. On the other hand, within the shot duration $\Delta\tau$ of a single spike displacement of material is only possible over a distance of the order $\delta \approx c_s \Delta\tau$. From electron temperature measurements[9] the sound velocity $c_s$ is typically $c_s \simeq 10^7$ cm sec$^{-1}$; hence with $\Delta\tau < 30$ psec one obtains $\delta < 3 \times 10^{-4}$ cm and $\delta \ll d$. Whereas local modulation of the plasma layer due to backscatter instabilities may thus well occur, macroscopic deformation of the plasma layer with classical mirror formation[4,8] has to be ruled out.

Thus, as regards the angular distribution of scattered radiation, experiment and simulations agree in that (i) part of the radiation is reflected specularly and is accompanied by specular SH emission, and that (ii) as a result of instability, radiation is scattered in the backward direction. Though not actually resolved, typical growth rates of the relevant instabilities of the order of $10^{12}$ sec$^{-1}$ are consistent with the measurements. As in the simulations, the scattered radiation peaks distinctly in the backward direction; thus, the highly ordered state of the perturbed plasma layer as seen in simulations and sketched in Fig. 2 should be relevant to reality. Without affecting this conclusion it should be mentioned that specularly reflected radiation could still be produced in the experiment after the onset of instability as zero-order scattering from the modulated plasma layer. Problems of this type could only be studied with equipment of considerably improved time resolution.

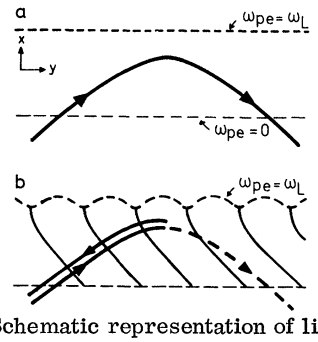


FIG. 2. Schematic representation of light ray propagation in (a) a smooth inhomogeneous plasma layer (specular reflections) and (b) a perturbed plasma layer (collimated backscatter). Curved solid lines in (b) are crests of ion sound waves; the dashed light ray in the specular direction represents zero-order scattering from an imperfectly "blazed" structure.

Backscatter from the perturbed plasma layer may be considered under two aspects, namely volume scattering by the underdense plasma and surfacelike scattering, similar to that from a blazed metal grating, by the modulated critical-density layer [see Fig. 2(b)]. These two aspects may be connected with stimulated Brillouin scattering (SBS)[2] and the radiative decay instability (RDI),[3] respectively. Although the mutual relation between these instabilities is not yet clear, some features of the experiment are more readily interpreted in terms of the latter instability. The RDI instability can occur in a modified, steplike density profile which may be generated in the vicinity of the critical layer by light pressure[3] and can account for the red shift of backscattered radiation[4] even with supersonic streaming on the low density side of the step. Furthermore, the RDI threshold condition $V_0/V_e > 5(k_0 L)^{1/2} \lambda_D / L$ taken together with the experimentally observed intensity dependence of the electron temperature, $T_e = T_0(\Phi/\Phi_0)^{0.3}$ where $T_0 = 400$ eV at $\Phi_0 = 10^{14}$ W cm$^{-2}$, suggests threshold intensities even below the threshold intensity for plasma production ($10^9$–$10^{10}$ W cm$^{-2}$). This is consistent with the fact that no indications of a threshold for collimated backscatter have ever been observed in our experiment down to the lowest applied intensities of $\simeq 10^{12}$ W cm$^{-2}$. A certain discrepancy with the threshold intensity of $\simeq 10^{13}$ W cm$^{-2}$ estimated at NRL[10] remains unexplained. Probably it is not due to the presence of spikes in the beam since a recent investigation using the same laser system has shown a very pronounced threshold behavior for $\frac{3}{2}\omega_L$ emission at a time-averaged intensity which is in good agreement with the theoretical threshold for the $2\omega_{pe}$ instability.[11]

Finally, the exemplary rather than singular character of the examples presented here should be emphasized. Differences in the relative intensity of collimated and specular backscatter[4] now appear as consequences of widely differing plasma parameters and shape on irradiation of various targets with varying intensity and focusing conditions. Furthermore, there are an increasing number of experiments with Nd,[6] $CO_2$,[7] and ruby[8] lasers where the observations seem to indicate that similar phenomena are encountered. Thus, laser light propagation in an unstable plasma layer may proceed qualitatively as described here for broad ranges of intensity and wavelength.

The authors are indebted to D. Biskamp, D. W. Forslund, and P. Mulser for discussions. This

work was performed under the terms of the agreement on association between Max-Planck-Institut für Plasmaphysik and EURATOM.

*On leave from Bhabha Atomic Research Center, Bombay, India.

[1]V. L. Ginzburg, *The Propagation of Electromagnetic Waves in Plasmas* (Pergamon, New York, 1964), p. 213.

[2]D. Biskamp and H. Welter, in *Plasma Physics and Controlled Nuclear Fusion* (International Atomic Energy Agency, Vienna, Austria, 1975), Vol. II, p. 507.

[3]D. W. Forslund, J. M. Kindel, Kenneth Lee, and E. L. Lindman, Phys. Rev. Lett. 34, 193 (1975).

[4]K. Eidmann and R. Sigel, in *Laser Interaction and Related Phenomena*, edited by H. J. Schwarz and H. Hora (Plenum, New York, 1974), Vol. 3, p. 667.

[5]K. Eidmann and R. Sigel, Phys. Rev. Lett. 34, 799 (1975).

[6]J. W. Shearer, S. W. Mead, J. Petruzzi, F. Rainer, J. E. Swain, and C. E. Violet, Phys. Rev. A 6, 764 (1972); A. Saleres, F. Floux, D. Cognard, and J. L. Bobin, Phys. Lett. 45A, 451 (1973); P. Lee, D. V. Giovanelli, R. P. Godwin, and G. H. McCall, Appl. Phys. Lett. 24, 406 (1974); B. H. Ripin, J. M. McMahon, E. A. McLean, W. M. Manheimer, and J. A. Stamper, Phys. Rev. Lett. 33, 634 (1974); M. Lubin, E. Goldman, J. Soures, L. Goldman, W. Friedman, S. Letzring, J. Albritton, P. Koch, and B. Yaakobi, in *Plasma Physics and Controlled Nuclear Fusion* (International Atomic Energy Agency, Vienna, 1975), Paper No. IAEA-CN-33/F4-2.

[7]K. B. Mitchell, T. F. Stratton, and P. B. Weiss, Appl. Phys. Lett. 27, 11 (1975).

[8]E. Jannitti, A. M. Malvezzi, and G. Tondello, J. Appl. Phys. 46, 3096 (1975).

[9]M. H. Key, K. Eidmann, C. Dorn, and R. Sigel, Phys. Lett. 48A, 121 (1974); C. G. M. van Kessel and R. Sigel, Phys. Rev. Lett. 33, 1020 (1974).

[10]Ripin *et al.*, Ref. 6.

[11]H. C. Pant, K. Eidmann, P. Sachsenmaier, and R. Sigel, Opt. Commun. 16, 396 (1976).

# Dynamics of Entropy Fluctuations in a Critical Binary Mixture

P. Calmettes and C. Laj

*Service de Physique du Solide et de Résonance Magnétique, Centre d'Etudes Nucléaires de Saclay, 91190 Gif-sur-Yvette, France*

(Received 15 September 1975)

Using a very sophisticated light-beating spectrometer and a new correlation technique, we have measured the relaxation time of entropy fluctuations in a critical binary mixture in the reduced temperature range of $4\times10^{-6}\leq t\leq10^{-1}$. In the hydrodynamic regime this relaxation time, which is proportional to the specific heat at constant pressure and critical concentration, is found to behave as $t^{-\alpha}(1+Bt^{+x})$ with a critical exponent $\alpha=0.059\pm0.003$ and $x=1.05\pm0.15$.

Light-beating spectroscopy has provided numerous important results regarding the dynamics of concentration fluctuations in liquid mixtures especially near the critical point. As a result of both the strong divergence of the intensity of the light scattered from these fluctuations and their critical slowing down, large signal-to-noise ratios can be achieved which allow a precise determination of the decay rate of concentration fluctuations $\Gamma_c$.

In critical binary mixtures the dynamics of entropy fluctuations is basically as important as the dynamics of concentration fluctuations. In the hydrodynamic regime, the decay rate of entropy fluctuations is $\Gamma_s'=D_s'q^2$ where $q$ is the wave number of fluctuations and $D_s'$ is a diffusion coefficient given by the ratio of $\Lambda'$, a noncritical kinetic coefficient, to $C_{p,c}$ the specific heat per unit volume, at constant pressure and critical concentration.

Because of the coupling between entropy and concentration fluctuations, $\Lambda'$ is slightly larger than the thermal conductivity $\Lambda$, except at the critical point where $\Lambda=\Lambda'$.[1] As the temperature $T$ approaches $T_c$, $C_{p,c}$ is theoretically expected to follow the temperature dependence

$$C_{p,c}=At^{-\alpha}[1+Bt^{x}]+C,$$

where $t=\Delta T/T_c=(T-T_c)/T_c$. $At^{-\alpha}$ describes the asymptotic behavior of the specific heat and $Bt^x$ is the first nonanalytic correction term predicted by renormalization-group theory.[2] The coefficients $A$, $B$ and the regular part $C$ of $C_{p,x}$ may be weakly temperature dependent (analytic functions of $t$). The critical exponent $\alpha$ and the subcritical one $x$ are expected to be about 0.125 and 0.640,[3] respectively, for the three-dimensional Ising model.

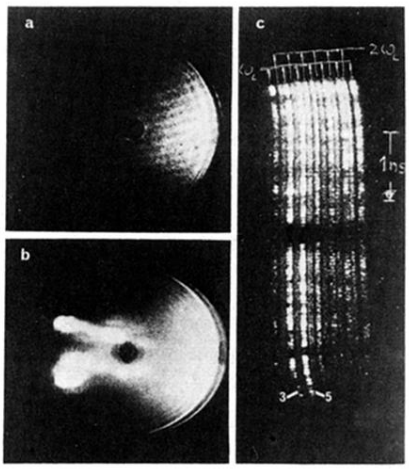


FIG. 1. Photographs of the focusing lens in the light of backscattered radiation. (a), (b) Time-integrated photographs at frequencies $2\omega_L$ and $\omega_L$, respectively. (c) Streak photograph with streak slit horizontal through the center of the lens. Channels three and five monitor collimated backscatter from two hot spots as seen in (b).